October 2007 Volume 3 Issue 3

Trade Science Inc.

Macromolecules

An Indian Journal

Full Paper

MMAIJ, 3(3), 2007 [119-127]

Hybrid Numerical Method For Studying Thermal Deformation In Rotating Multilayered Hollow Cylinder

Z.Y.Lee*[1], C.C.Wang[2], H.M.Sung[1], C.Y.Hu[3]

[1]Department of Mechanical Engineering, Hsiuping Institute of Technology, Taichung, 412, (TAIWAN)

[2]Department of Information Management, Hsing kuo University of Management, Tainan, 701, (TAIWAN)

[3]Liberal Arts Center, University of Da-Yeh, Tsuen, Changhua, 515, (TAIWAN)

Tell: +886-4-24961123ext1103 ; Fax: +886-4-24961108

E-mail : zylee@mail.hit.edu.tw

Received: 27th September, 2007 ; Accepted: 2nd October, 2007

ABSTRACT

This paper deals with the quasi-static coupled thermoelastic problems of an infinitely long rotating multilayered hollow cylinder. Laplace transform and finite difference methods are used to analyze problems. Using the Laplace transform with respect to time, the general solutions of the governing equations are obtained in transform domain. The solution is obtained by using the matrix similarity transformation and inverse Laplace transform. Also presented are the numerically transient distributions of stress and temperature in the real domain for the case of an infinitely long rotating hollow cylinder composed of three different materials. Moreover, the computational procedures established in this article can solve the generalized thermoelasticity problem for rotating multilayered hollow cylinder with orthotropic material properties.

KEYWORDS

Multilayered;
Laplace transform;
Similarity transformation.

INTRODUCTION

Durodola and Attia[1] are a predictive assessment of the stresses in and deformation of a rotating disc made of functionally graded non-homogeneous orthotropic materials. Two methods of analysis, namely, the finite-element method and direct numerical integration of governing differential equations were used. Lee et al.[2] analyze the free vibration and transient dynamic response of a rotating multilayer annular plate. Layerwise zig-zag theory is applied to the rotating multilayer disk problem. Kant et al.[3] analyzed the transient response of composite and sandwich plates based on a equivalent single-layer higher-order theory.

Chen et al.[4,5] presented a new numerical technique hybrid numerical method for the problem of a transient linear heat conduction system. They applied the Laplace transform to remove the time-dependence from the governing equation and boundary conditions, and solved the transformed equations with the finite element and finite difference method. Finally the transformed temperature was inverted by numerical inversion of the laplace transform. It proved that the method could accurately determine the stable solutions at a specific time. But this method

has been confined to one nodal solution at each specific time. When applied to a problem with many nodes, it takes an excessive amount of computer time. Yang and Chen[6] discussed the transient response of one-dimensional quasi-static coupled thermoelasticity problems of an infinitely long annular cylinder composed of two different materials. They applied the laplace transform with respect to time and used the fourier series and matrix operations to obtain the solution.

In this paper, we consider the one-dimensional quasi-static coupled thermoelastic problem of rotating multilayered hollow cylinder. Laplace transforms and finite difference methods are used, which are quite effective and powerful for obtaining solutions to a wide range of transient thermal stress.

FORMULATION

The layered cylindrical shell to be analyzed is shown in figure 1. The transient heat conduction equation for the ith layer in dimensional form can be written as

$$[k_r \frac{\partial^2}{\partial r^{*2}} + k_\theta \frac{1}{r^*}\frac{\partial}{\partial r^*}]\overline{\Theta} = \rho C_v \frac{\partial \overline{\Theta}}{\partial \tau} + \Theta_0 \beta_r \frac{\partial}{\partial r^*}(\frac{\partial U}{\partial \tau}) + \Theta_0 \beta_\theta \frac{1}{r^*}(\frac{\partial U}{\partial \tau}) \quad (1)$$

Where $\overline{\Theta} = \Theta - \Theta_0$, $\beta_r = \frac{E_r}{1-\nu_{r\theta}\nu_{\theta r}}(\alpha_r + \nu_{\theta r}\alpha_\theta)$ and

$$\beta_\theta = \frac{E_\theta}{1-\nu_{r\theta}\nu_{\theta r}}(\alpha_\theta + \nu_{r\theta}\alpha_r)$$

The equation of equilibrium for a cylinder along the radial direction can be written as

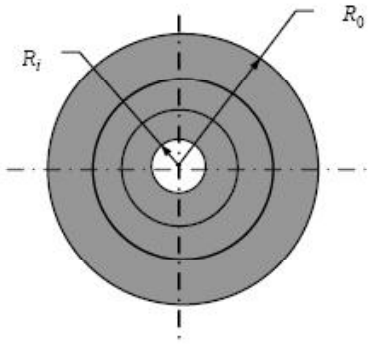

Figure 1 : Physical model and system ordinates for a Multilayered hollow cylinder

$$\frac{\partial^2 U}{\partial r^{*2}} + [\frac{E_\theta}{E_r}\nu_{\theta r} + (1-\nu_{r\theta})]\frac{1}{r^*}\frac{\partial U}{\partial r^*} - \frac{E_\theta}{E_r}\frac{1}{r^{*2}}$$

$$U = (\alpha_r + \nu_{\theta r}\alpha_\theta)\frac{\partial \overline{\Theta}}{\partial r^*} - [\frac{E_\theta}{E_r}(\alpha_\theta + \nu_{r\theta}\alpha_r) - (\alpha_r + \nu_{\theta r}\alpha_\theta)]\frac{\overline{\Theta}}{r^*} - \frac{\lambda \rho w^2 r^*}{E_r} \quad (2)$$

The stress-displacement relations are

$$\sigma^*_{ri} = (\frac{E_r}{\lambda})_i \frac{\partial U}{\partial r^*} + (\frac{E_\theta \nu_{\theta r}}{\lambda})_i \frac{U}{r^*} - \beta_{ri}(\Theta - \Theta_0) \quad (3)$$

$$\sigma^*_{\theta i} = (\frac{E_r \nu_{r\theta}}{\lambda})_i \frac{\partial U}{\partial r^*} + (\frac{E_\theta}{\lambda})_i \frac{U}{r^*} - \beta_{\theta i}(\Theta - \Theta_0) \quad (4)$$

Let the boundary surfaces of composite cylinder be traction free and subjected to temperatures. The initial and boundary conditions are

Case 1

$U = \dot{U} = \overline{\Theta} = \dot{\overline{\Theta}} = 0$ at $t = 0$

$\sigma^*_r(r^*, \tau) = 0$ at $r^* = R_1$

$\Theta_1 - \Theta_0 = f_1$ at $r^* = R_1$

$\sigma^*_r(r^*, \tau) = 0$ at $r^* = R_{out}$

$\frac{\partial \Theta}{\partial r^*} = 0$ at $r^* = R_{out}$

Case 2

$U = \dot{U} = \overline{\Theta} = \dot{\overline{\Theta}} = 0$ at $t = 0$

$\sigma^*_r(r^*, \tau) = 0$, at $r^* = R_1$

$\Theta_1 - \Theta_0 = f_1$ at $r^* = R_1$

$\sigma^*_r(r^*, \tau) = 0$ at $r^* = R_{out}$

$-k\frac{\partial \Theta}{\partial r^*} = h(\Theta - \Theta_\infty)$ at $r^* = R_{out}$

At the interface between two adjacent layers, the following matching conditions must be satisfied

$U_i(r^*, \tau) = U_{i+1}(r^*, \tau)$ $r^* = R_i$

$\sigma^*_{ri}(r^*, \tau) = \sigma_{ri+1}(r^*, \tau)$ $r^* = R_i$

$q_i = q_{i+1}$ $r^* = R_i$

$\overline{\Theta}_i(r^*, \tau) = \overline{\Theta}_{i+1}(r^*, \tau)$ $r^* = R_i$

$i = 1, 2, ..., m-1$

The non-dimensional variables are defined as fol-

lows:

$$T = (\Theta - \Theta_0)/\Theta_0 = \overline{\Theta}/\Theta_0 \qquad a_i = (\frac{k_r}{\rho C_v})_i \Big/ (\frac{k_r}{\rho C_v})_1$$

$$b_i = (\frac{k_\theta}{\rho C_v})_i \Big/ (\frac{k_r}{\rho C_v})_1 \qquad w_i = (\frac{\beta_\theta}{\rho C_v})_i \Big/ (\frac{\beta_r}{\rho C_v})_i$$

$$t = (\frac{k_r}{\rho C_v})_1 \tau \Big/ R_1^2 \qquad r = r^* / R_1$$

$$u = U(\frac{\beta_r}{\rho C_v})_1 \Big/ R_1 \qquad e_i = [\nu_{\theta r} E_\theta / E_r + (1 - \nu_{r\theta})]_i$$

$$f_i = (E_\theta / E_r)_i \qquad {}_1Q_i = (\frac{E_r}{\lambda})_i \Big/ [\beta_{r1}(\frac{\beta_r}{\rho C_v})_i \Theta_0]$$

$${}_2Q_i = (\frac{E_\theta \nu_{\theta r}}{\lambda})_i \Big/ [\beta_{r1}(\frac{\beta_r}{\rho C_v})_i \Theta_0] \qquad {}_3Q_i = \beta_{ri}/\beta_{r1}$$

$${}_1R_i = (\frac{E_r \nu_{r\theta}}{\lambda})_i \Big/ [\beta_{\theta 1}(\frac{\beta_r}{\rho C_v})_i \Theta_0]$$

$${}_2R_i = (\frac{E_\theta}{\lambda})_i \Big/ [\beta_{\theta 1}(\frac{\beta_r}{\rho C_v})_i \Theta_0]$$

$${}_3R_i = \beta_{\theta i}/\beta_{\theta 1} \qquad \sigma_{ri} = \sigma_{ri}^* / (\beta_{r1}\Theta_0)$$

$${}_3R_i = \beta_{\theta i}/\beta_{\theta 1} \qquad \sigma_{ri} = \sigma_{ri}^* / (\beta_{r1}\Theta_0)$$

$$\sigma_{\theta i} = \sigma_{\theta i}^* / (\beta_{\theta 1}\Theta_0) \qquad h_i = (\frac{\beta_r}{\rho C_v})_i [\frac{E_\theta}{E_r}(\alpha_\theta + \nu_{r\theta}\alpha_r) - (\alpha_r + \nu_{\theta r}\alpha_\theta)]_i \Theta_0$$

$$k_i = [\frac{\lambda \rho^2 C_v w^2}{E_r \beta_r}]_i \qquad (5)$$

Substituting the nondimensional quantities given in equation (5) into the governing equations (1)-(4), the governing equations and stress-displacement relations have the following nondimensional form:

$$\{ [a_i \frac{\partial^2}{\partial r^2} + \frac{b_i}{r}\frac{\partial}{\partial r}] - \frac{\partial}{\partial t} \} T = \frac{\partial}{\partial r}(\frac{\partial u}{\partial t}) + \frac{w_i}{r}(\frac{\partial u}{\partial t}) \qquad (6)$$

$$\frac{\partial^2 u}{\partial r^2} + \frac{e_i}{r}\frac{\partial u}{\partial r} - f_i \frac{u}{r^2} = g_i \frac{\partial T}{\partial r} - h_i \frac{T}{r} - k_i r \qquad (7)$$

$$\sigma_{ri} = {}_1Q_i \frac{\partial u}{\partial r} + {}_2Q_i \frac{u}{r} - {}_3Q_i T \qquad (8)$$

$$\sigma_{\theta i} = {}_1R_i \frac{\partial u}{\partial r} + {}_2R_i \frac{u}{r} - {}_3R_i T \qquad (9)$$

The nondimensional boundary and interface conditions can be written as:

Boundary conditions

Case 1

$\sigma_r(r,t) = 0$ at $r = r_1$

$T_1 = f_1/\Theta_0$ at $r = r_1$

$\sigma_r(r,t) = 0$ at $r = r_{out}$

$\frac{\partial T}{\partial r} = 0$ at $r = r_{out}$

Case 2

$\sigma_r(r,t) = 0$, at $r = r_1$

$T_1 = f_1/\Theta_0$ at $r = r_1$

$\sigma_r(r,t) = 0$ at $r = r_{out}$

$-k\frac{\partial T}{\partial r} = h(T - T_\infty)$ at $r = r_{out}$

2. Interface conditions

$u_i(r,t) = u_{i+1}(r,t)$ $r = r_{i+1}$

$\sigma_{ri}(r,t) = \sigma_{ri+1}(r,t)$ $r = r_{i+1}$

$q_i = q_{i+1}$ $r = r_{i+1}$

$T_i(r,t) = T_{i+1}(r,t)$ $r = r_{i+1}$

$i = 1,2,...,m-1$ layer

Applying central difference in equations (6), (7), (8) and (9), we obtain the following discretized equations:

$$a_i \frac{T_{j+1} - 2T_j + T_{j-1}}{(\Delta r_i)^2} + b_i \frac{1}{r_j}\frac{T_{j+1} - T_{j-1}}{2\Delta r_i} - \frac{\partial T_j}{\partial t} = \frac{w_i}{r_j}\frac{\partial u_j}{\partial t} + \frac{(\frac{\partial u}{\partial t})_{j+1} - (\frac{\partial u}{\partial t})_{j-1}}{2\Delta r_i} \qquad (10)$$

$$\frac{u_{j+1} - 2u_j + u_{j-1}}{(\Delta r_i)^2} + e_i \frac{1}{r_j}\frac{u_{j+1} - u_{j-1}}{2\Delta r_i} - f_i \frac{1}{r_j^2} u_j = g_i \frac{T_{j+1} - T_{j-1}}{2\Delta r_i} - h_i \frac{T_j}{r_j} - k_i r_j \qquad (11)$$

$$\sigma_{ri} = {}_1Q_i \frac{u_{j+1} - u_{j-1}}{2\Delta r_i} + {}_2Q_i \frac{u_j}{r_j} - {}_3Q_i T_j \qquad (12)$$

$$\sigma_{\theta i} = {}_1R_i \frac{u_{j+1} - u_{j-1}}{2\Delta r_i} + {}_2R_i \frac{u_j}{r_j} - {}_3R_i T_j \qquad (13)$$

where $\Delta r_i = (r_{i+1} - r_i)/(\eta - 1)$ and n is number of grid point for each layer.

The Laplace transform of a function $\Phi(t)$ and its inverse are defined by

$$\overline{\Phi}(s) = L[\Phi(t)] = \int_0^\infty e^{-st}\Phi(t)dt$$

$$\Phi(t) = L^{-1}[\overline{\Phi}(s)] = \frac{1}{2\pi i}\int_{c-i\infty}^{c+i\infty} e^{st}\overline{\Phi}(s)ds$$

Taking the Laplace transform for equations (10), (11), (12) and (13), we obtain the following equations:

$$a_i\frac{\overline{T}_{j+1}-2\overline{T}_j+\overline{T}_{j-1}}{(\Delta r_i)^2}+b_i\frac{1}{r_j}\frac{\overline{T}_{j+1}-\overline{T}_{j-1}}{2\Delta r_i}-$$
$$(T_{j,in}+s\overline{T}_j)=\frac{w_i}{r_j}(u_{j,in}+s\overline{u}_j)$$
$$+\frac{1}{2\Delta r_i}\left[(u_{j+1,in}+s\overline{u}_{j+1})-(u_{j-1,in}+s\overline{u}_{j-1})\right] \quad (14)$$

$$\frac{\overline{u}_{j+1}-2\overline{u}_j+\overline{u}_{j-1}}{(\Delta r_i)^2}+e_i\frac{1}{r_j}\frac{\overline{u}_{j+1}-\overline{u}_{j-1}}{2\Delta r_i}-f_i\frac{1}{r_j^{\,2}}\overline{u}_j$$
$$=g_i\frac{\overline{T}_{j+1}-\overline{T}_{j-1}}{2\Delta r_i}-h_i\frac{\overline{T}_j}{r_j}-k_i r_j \quad (15)$$

Let the surface of the cylindrical inner surface be stress free and subject to a time-dependent temperature. After taking Laplace transformation, the boundary conditions in transformed domain become

Case 1

$$\overline{\sigma}_r(r,s)=0 \qquad \text{at } r=r_1$$
$$\overline{T}_1=\overline{f}_1(s)/\Theta_0 \qquad \text{at } r=r_1$$
$$\overline{\sigma}_r(r,s)=0, \qquad \text{at } r=r_{out}$$
$$\frac{\partial\overline{T}}{\partial r}=0 \qquad \text{at } r=r_{out}$$

Case 2

$$\overline{\sigma}_r(r,s)=0, \qquad \text{at } r=r_1$$
$$\overline{T}_1=\overline{f}_1(s)/\Theta_0, \qquad \text{at } r=r_1$$
$$\overline{\sigma}_r(r,s)=0, \qquad \text{at } r=r_{out}$$
$$-k\frac{\partial\overline{T}}{\partial r}=h(\overline{T}-\overline{T}_\infty), \qquad \text{at } r=r_{out} \quad (16)$$

The interface conditions are as follows:

$$\begin{aligned}&\overline{u}_i(r,s)=\overline{u}_{i+1}(r,s) \quad r=r_{i+1}\\ &\overline{\sigma}_{ri}(r,s)=\overline{\sigma}_{ri+1}(r,s) \quad r=r_{i+1}\\ &\overline{q}_i(r,s)=\overline{q}_{i+1}(r,s) \quad r=r_{i+1}\\ &\overline{T}_i(r,s)=\overline{T}_{i+1}(r,s) \quad r=r_{i+1}\end{aligned} \quad i=1,2,\ldots,m-1 \quad (17)$$

Substituting equations (16),(17) into equations (14),(15), we obtain the following equation in matrix form

$$\left\{\begin{bmatrix} B_1 & C_1 & & & \\ A_2 & B_2 & C_2 & & \\ & \ddots & \ddots & \ddots & \\ & & A_{N-1} & B_{N-1} & C_{N-1} \\ & & & A_N & B_N \end{bmatrix} - s[I]\right\}\begin{bmatrix} \overline{T}_1 \\ \overline{T}_1 \\ \vdots \\ \overline{T}_{N-1} \\ \overline{T}_N \end{bmatrix} + \quad (18)$$

$$s\begin{bmatrix} E_1 & F_1 & & & \\ D_2 & E_2 & F_2 & & \\ & \ddots & \ddots & \ddots & \\ & & D_{N-1} & E_{N-1} & F_{N-1} \\ & & & D_N & E_N \end{bmatrix}\begin{bmatrix} \overline{u}_1 \\ \overline{u}_1 \\ \vdots \\ \overline{u}_{N-1} \\ \overline{u}_N \end{bmatrix} = \begin{bmatrix} \overline{G}_1 \\ \overline{G}_1 \\ \vdots \\ \overline{G}_{N-1} \\ \overline{G}_N \end{bmatrix}$$

where

$$B_1=-[1+\frac{{}_3Q_1}{{}_1Q_1}]^{-1}[\frac{a_1}{(\Delta r_1)^2}] \quad C_1=[1+\frac{{}_3Q_1}{{}_1Q_1}]^{-1}[\frac{a_1}{(\Delta r_1)^2}+\frac{b_1}{r_1}\frac{1}{2\Delta r_1}]$$

$$A_j=\frac{a_i}{(\Delta r_i)^2}-\frac{b_i}{r_j}\frac{1}{2\Delta r_i} \qquad B_j=-\frac{2a_i}{(\Delta r_i)^2}$$

$$C_j=\frac{a_i}{(\Delta r_i)^2}+\frac{b_i}{r_j}\frac{1}{2\Delta r_i} \qquad E_1=[1+\frac{{}_3Q_1}{{}_1Q_1}]^{-1}[\frac{1}{r_1}\frac{{}_2Q_1}{{}_1Q_1}-\frac{w_1}{r_1}]$$

$$F_1=D_N=0 \qquad D_j=\frac{1}{2\Delta r_i}$$

$$A_N=[1+\frac{{}_3Q_m}{{}_1Q_m}]^{-1}[-\frac{a_m}{(\Delta r_m)^2}+\frac{b_m}{r_k}-\frac{b_m}{r_k}\frac{1}{2\Delta r_m}] \quad E_j=-\frac{w_i}{r_j}$$

$$B_N=-[1+\frac{{}_3Q_m}{{}_1Q_m}]^{-1}[\frac{2a_m}{(\Delta r_m)^2}] \qquad F_j=\frac{1}{2\Delta r_i}$$

$$E_N=[1+\frac{{}_3Q_m}{{}_1Q_m}]^{-1}[-\frac{w_m}{r_k}+\frac{{}_2Q_m}{{}_1Q_m}\frac{1}{r_k}] \qquad \overline{G}_j=0$$

$$\overline{G}_1=[1+\frac{{}_3Q_1}{{}_1Q_1}]^{-1}[(\frac{b_1}{r_1}\frac{1}{2\Delta r_1}-\frac{a_1}{(\Delta r_1)^2})T_1]$$

$$\overline{G}_N=-[1+\frac{{}_3Q_m}{{}_1Q_m}]^{-1}[(\frac{a_m}{(\Delta r_m)^2}+\frac{b_m}{r_k}\frac{1}{2\Delta r_m})T_{N+1}]$$

m denotes the last layer, k the last point and i denotes ith layer for j=2,3,…,N-1

$$\begin{bmatrix} l_1 & J_1 & & & \\ H_2 & l_2 & & & \\ & \ddots & \ddots & \ddots & \\ & & H_{N-1} & l_{N-1} & J_{N-1} \\ & & & H_N & l_N \end{bmatrix}\begin{bmatrix} T_1 \\ T_1 \\ \vdots \\ T_{N-1} \\ T_N \end{bmatrix} +$$

$$\begin{bmatrix} L_1 & M_2 & & & & \\ K_2 & L_1 & M_2 & & & \\ & \ddots & \ddots & \ddots & & \\ & & K_{N-1} & L_{N-1} & M_{N-1} & \\ & & & L_N & L_N & \end{bmatrix} \begin{bmatrix} \bar{u}_1 \\ \bar{u}_2 \\ \vdots \\ \bar{u}_{N-1} \\ \bar{u}_N \end{bmatrix} = \begin{bmatrix} \bar{V}_1 \\ \bar{V}_2 \\ \vdots \\ 0 \\ \bar{V}_N \end{bmatrix} + \begin{bmatrix} \bar{V}_1 \\ \bar{V}_2 \\ \vdots \\ \vdots \\ \bar{U}_N \end{bmatrix} \quad (19)$$

where

$$I_1 = \frac{{}_3Q_1}{{}_1Q_1}\left(\frac{e_1}{r_1} - \frac{2}{\Delta r_1}\right) + \frac{h_1}{r_1} \qquad J_1 = -\frac{g_i}{2\Delta r_i}$$

$$I_j = \frac{h_i}{r_j} \qquad J_j = -\frac{g_i}{2\Delta r_i}$$

$$L_1 = \frac{{}_2Q_1}{{}_1Q_1}\left(\frac{2}{r_1\Delta r_1} - \frac{e_1}{r_1^2}\right) - \frac{2}{(\Delta r_1)^2} - \frac{f_1}{r_1^2} \qquad H_j = \frac{g_i}{2\Delta r_i}$$

$$M_1 = \frac{2}{(\Delta r_j)^2} \qquad K_j = \frac{1}{(\Delta r_j)^2} - \frac{e_i}{r_j}\frac{1}{2\Delta r_i}$$

$$H_N = \frac{g_m}{2\Delta r_{mi}} \qquad L_j = -\frac{2}{(\Delta r_i)^2} + \frac{f_i}{r_j^2}$$

$$I_N = \frac{{}_3Q_m}{{}_1Q_{m1}}\left(\frac{e_m}{r_{m1}} + \frac{2}{\Delta r_m}\right) + \frac{h_{m1}}{r_{m1}} \qquad M_j = \frac{1}{(\Delta r_j)^2} + \frac{e_i}{r_j}\frac{1}{2\Delta r_i}$$

$$K_N = \frac{2}{(\Delta r_m)^2} \qquad \bar{V}_j = 0$$

$$\bar{U}_j = -k_i r_j \qquad L_N = \frac{{}_2Q_m}{{}_1Q_{m1}}\left(\frac{-2}{r_m\Delta r_{m1}} - \frac{e_m}{r_m^2}\right) - \frac{2}{(\Delta r_m)^2} - \frac{f_m}{r_m^2}$$

$$\bar{V}_1 = -\frac{g_1}{2\Delta r_1}T_1 \qquad \bar{V}_N = -\frac{g_{m1}}{2\Delta r_m}T_{N+1}$$

Equations (18) and (19) can be rewritten in the following matrix forms

$$\{[M] - s[I]\}\{\bar{T}_j\} + s[N]\{\bar{u}_j\} = \{\bar{G}_j\} \quad (20)$$

$$[R]\{\bar{T}_j\} + [Q]\{\bar{u}_j\} = \{\bar{V}\} + \{\bar{U}\} \quad (21)$$

where the matrices [M], [N], [R] and [Q] are the corresponding matrix in equations (18) and (19).

Substituting equation (21) into (20), we have

$$\{[A] - s[I]\}\{\bar{T}_j\} = \{\bar{F}_j\} \quad (22)$$

where

$$[A] = \{[N]^{-1} + [Q]^{-1}[R]\}^{-1}[N]^{-1}[M]$$

$$[F_j] = \{[N]^{-1} + [Q]^{-1}[R]\}^{-1}\{[N]^{-1} - s[Q]^{-1}\{[\bar{V}] + [\bar{U}]\}\}$$

Since the(N×N) matrix[A] is a nonsingular real matrix, the matrix[A] possesses a set of N linearly independent eigenvectors, hence the matrix [A] is diagonalizable. There exists a nonsingular transition matrix [P]such that$[P]^{-1}[A][P]$=diag [A], that is, the matrices[A] and diag [A] are similar, where the matrix diag [A] is defined as

$$\mathbf{diag}[A] = \begin{bmatrix} \lambda_1 & & & \\ & \lambda_2 & & \\ & & \ddots & \\ & & & \lambda_N \end{bmatrix} \quad (23)$$

where λ_j(j=1,2,…N) is the eigenvalue of matrix [A].

Substituting equation (23) into (22), we obtain the equation

$$\{[P]^{-1}[A][P] - s[P]^{-1}[I][P]\}[P]^{-1}\{\bar{T}_j\} = [P]^{-1}\{\bar{F}_j\} \quad (24)$$

Equation (24) can be rewritten as

$$\{\mathbf{diag}[A] - s[I]\}\{\bar{T}_j^*\} = \{\bar{F}_j^*\} \quad (25)$$

where

$$\{\bar{T}_j^*\} = [P]^{-1}\{\bar{T}_j\}$$

$$\{\bar{F}_j^*\} = [P]^{-1}\{\bar{F}_j\}$$

From equation (25), the following solutions can be obtained immediately.

$$\bar{T}_j^* = \frac{\bar{F}_j^*}{\lambda_j - s} \quad j = 1,2,..,N \quad (26)$$

By applying the inverse Laplace transform to equation (26), we get the solution T_j. After we have obtained T_j, then we can use following equations (27) and (28) to obtain the solutions T_j and u_j

$$\{T_j\} = [P]\{T_j^*\} \quad (27)$$

$$\{u_j\} = [Q]^{-1}\{[\bar{V}] + [\bar{U}]\} - [Q]^{-1}[R]\{T_j\} \quad (28)$$

NUMERICAL RESULTS AND DISCUSSIONS

In this study, we present some numerical results of the temperature distribution in a rotating multilayered composite hollow cylinder, and displacement and thermal stresses under temperature and angular velocity changes.

To illustrate the foregoing analysis, we performed numerical calculations for a rotating cylinder under an axisymmetric heating at the inner surface. For an infinitely long rotating multilayered cylinder, the geometry and material quantities of the cylinder are shown in

TABLE 1 : The geometry and material constants (R_{out}/R_1=4.5, h=200(watt/m^2.k), Θ_0=T∞298K)

	layer 1 titanium	layer 2 Al_2O_3
$E_\gamma=E_\theta$(N/m^2)	108E9	390E9
$k_\gamma=k_\theta$ (watt/m.k)	20	6
$\nu_{\gamma\theta}=\nu_{\theta\gamma}$	0.3	0.23
$\alpha_\gamma=\alpha_\theta$(1/K)	11E-6	8E-6
ρ(kg/m^3)	4	3.99
C_v(kJ/kg-K)	0.4	1.25

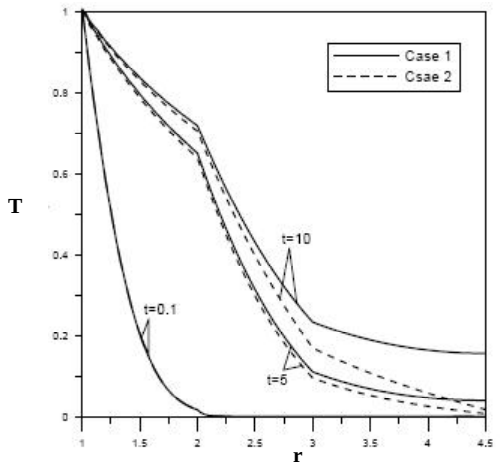

Figure 2 : Temperature distribution along radial direction for angular velocity w=10

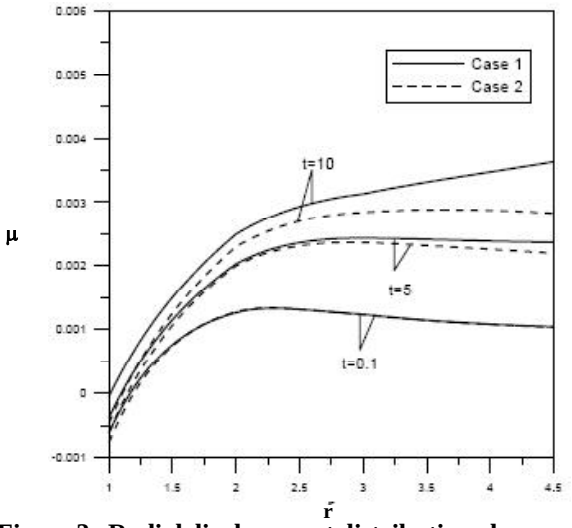

Figure 3 : Radial displacement distribution along radial direction for angular velocity w=10

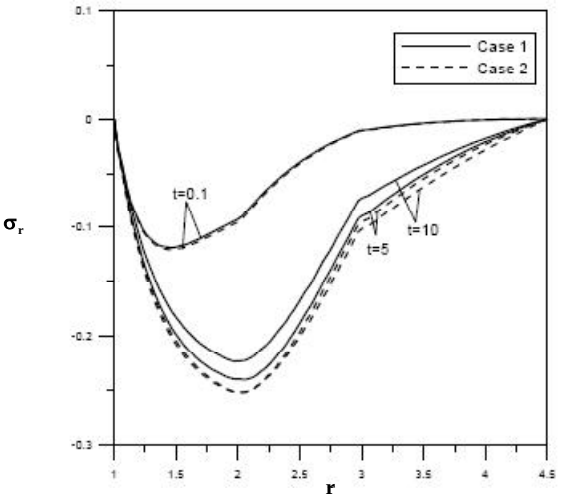

Figure 4 : Radial stress distribution along radial direction for angular velocity w=10

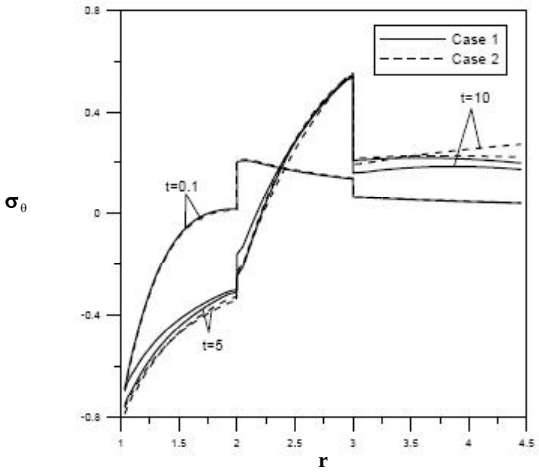

Figure 5 : Circumferential stress along radial direction for angular velocity w=10

TABLE 1. The inner and outer radius of the cylinder are assumed to be 1.0 and 4.5 respectively. The case 1 boundary conditions at inner and outer surfaces are assumed to be 1 and adiabatic respectively. The case 2 boundary conditions at inner and outer surfaces are assumed to be 1 and convection respectively. Each layer is assumed to have a different thickness (in the case of three layers, Δh_1=1, Δh_2=1, and Δh_3=1.5). Figures 2-5 show some numerical results of three layered cylinders for angular velocity ω=10 at time step t=0.1, 5 and 10. Figures 6-11 show some numerical results of three layered cylinders for different angular velocity at time step t=0.1, 1 and 10.

Figure 2 shows the temperature distributions along radial direction of angular velocity w=10 at t=0.1, 5 and 10 for adiabatic and convection boundary conditions. Figure 3 shows the variation of displacement along the radial direction. The results show that when the time step increases, the displacement distribution changes.

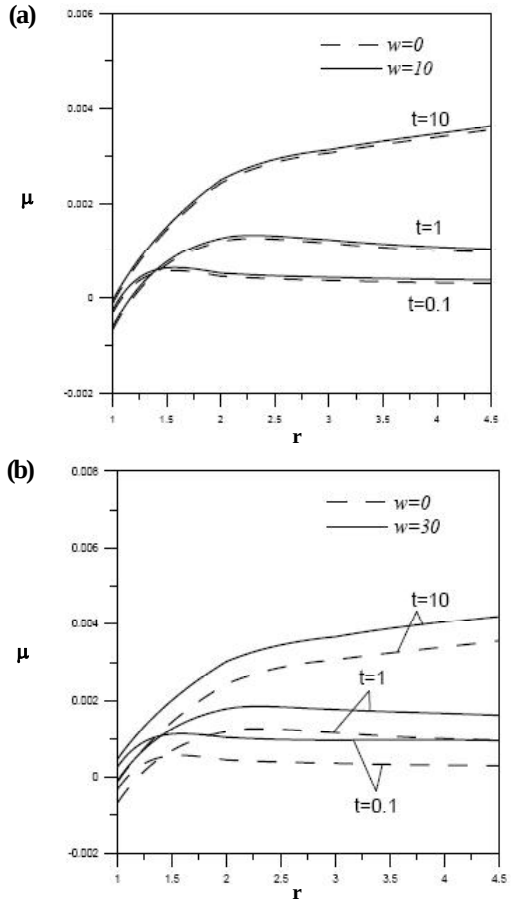

Figure 6 : Radial displacement distribution along radial direction and outer boundary being adiabatic

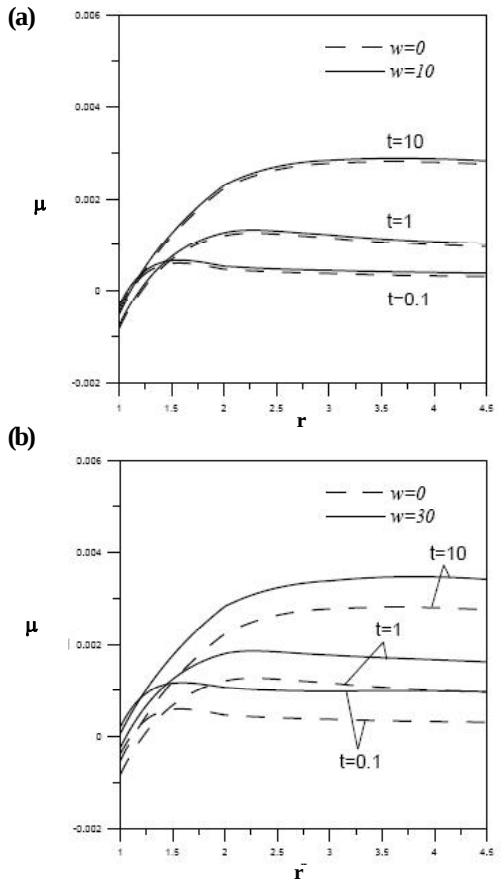

Figure 7 : Radial displacement distribution along radial direction and outer boundary being convection

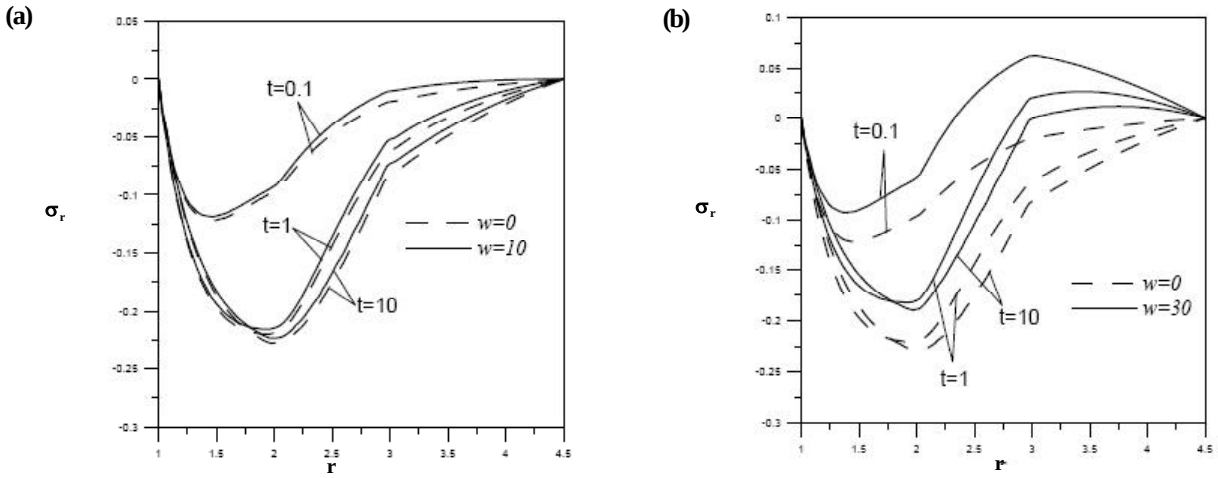

Figure 8 : Radial stress distribution along radial direction and outer boundary being adiabatic

Figure 4 shows the thermal radial stress distribution στ along the radial direction for different time step and boundary conditions. From this figure, we can see where the maximum radial stress may occur. However the circumferential stress has a significant jump at all interfaces as shown in figure 5. Figures 6 and 7 show the variation of displacement along the radial direction. The results show that when the angular velocity increases, the displacement distribution changes. Figures 8 and 9 show the thermal radial stress distribution στ along the

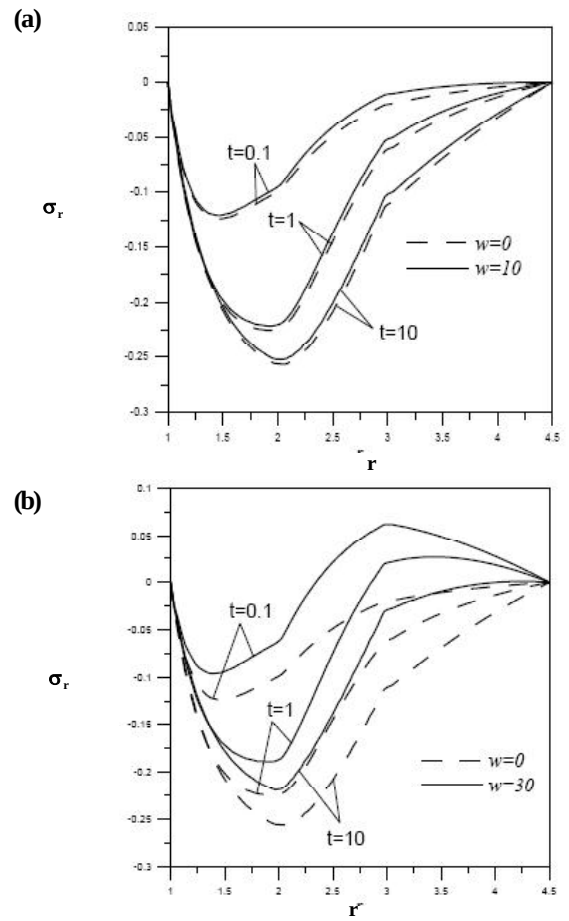

Figure 9 : Radial stress distribution along radial direction and outer boundary being convection

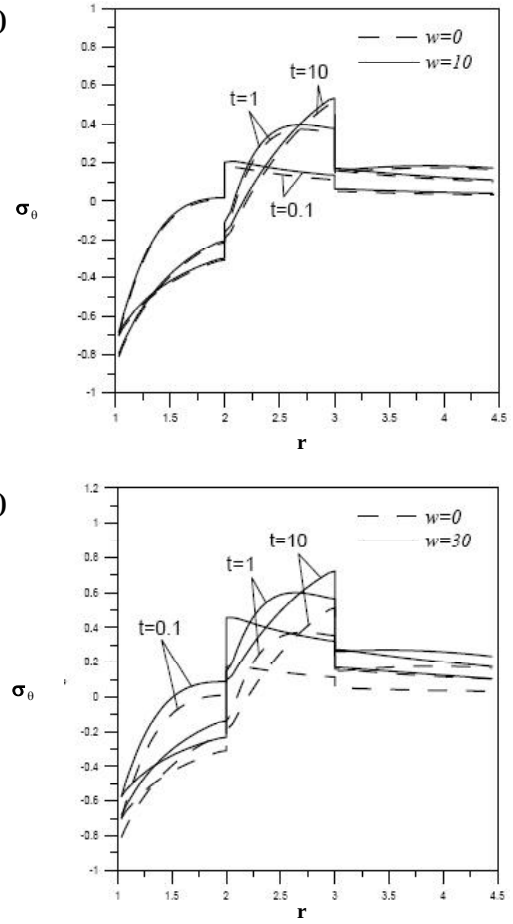

Figure 10 : Circumferential stress along radial direction and outer boundary being adiabatic

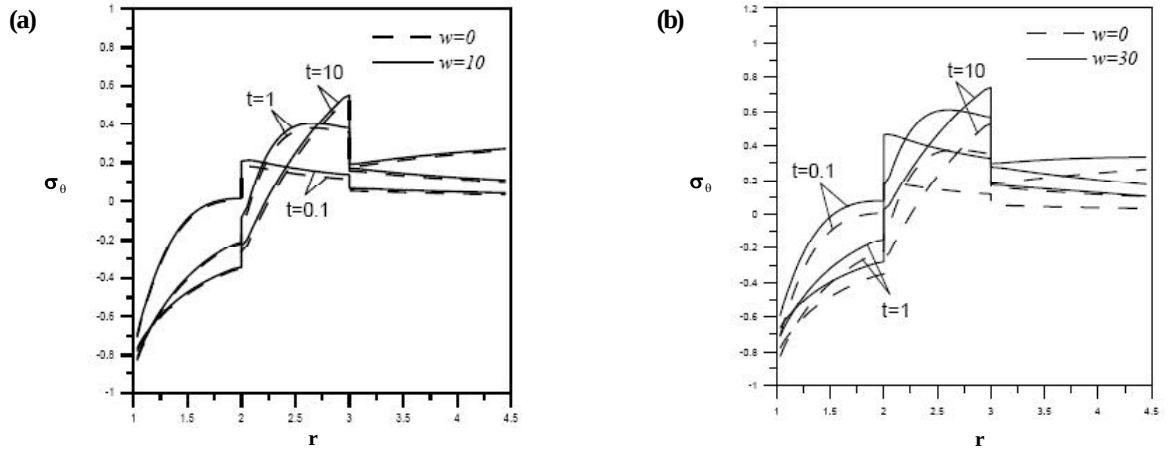

Figure 11 : Circumferential stress along radial direction and outer boundary being convection

radial direction for different angular velocity and boundary conditions. From this figure, we can see where the maximum radial stress may occur. However the circumferential stress has a significant jump at all interfaces as shown in figures 10 and 11. The discontinuity of thermal stress was due to the differences in material properties such as the coefficient of linear thermal expansion and Young's modulus. The thermal stress var-

ies characteristically in each layer, especially for the occurrence of discontinuities at all interfaces as shown in the figures 10 and 11.

CONCLUSIONS

In this paper, we discussed the thermoelastic transient response of rotating multilayered hollow cylinder whose outer surfaces are subjected to known adiabatic and convection. The one-dimensional quasi-static axisymmetric coupled thermoelastic problem of an infinitely long rotating hollow cylinder composed of multilayers of different ceramic-metal materials was discussed.

In the case of rotating multilayered hollow cylinder, the coupled term and angular velocity in generalized thermoelasticity formulation was discussed. From these figures, it should be concluded that the angular velocity effect behaves as a clear lag in both the displacement and the stress distributions with time. This means that the angular velocity increases displacement rise, and the thermal stresses are changed. It was found that the circumferential stress along radial direction is much larger than radial stress. The numerical results were obtained which can be applied to mechanical parts in precision measurement or design useful structural applications.

One advantage of hybrid numerical method is that the demands on computer memory are less than those required when applying the iteration method. The hybrid numerical method is of high efficiency and accuracy, and capable of eliminating numerical diffusion and oscillation effectively. This paper has been used to solve the simple problems selected from applications in rotating multilayered hollow cylinder. Similar behavior was found for a more difficult example. The proposed method may be easily extended to solve a wide range of physical engineering problems.

NOTATION

ρ	density
C_v	specific heat
k	thermal conductivity
α	linear thermal expansion coefficient
E	Young's modulus
ν	Poisson's ratio
Θ_0	reference temperature
Θ,T	dimensional and non-dimensional temperature
U,μ	dimensional and non-dimensional radial component of displacement
γ^*,r	dimensional and non-dimensional radial coordinate
τ,t	dimensional and non-dimensional time
$\sigma^*\gamma$	dimensional radial stress
$\sigma\gamma$	non-dimensional radial stress
$\sigma^*\theta$	dimensional circumferential stress
$\sigma\theta$	non-dimensional circumferential stress
q	heat flux in the radial direction
w	angular velocity

REFERENCES

[1] J.F.Durodola, O.Attia; Composites Science and Technology, **60**, 987 **(2000)**.

[2] D.Lee, A.M.Waas, B.H.Karnopp; Computer and structures, **66**, 313 **(1998)**.

[3] T.Kant, C.P.Arora, J.H.Varaiya; Composite structures, **22**, 109 **(1992)**.

[4] C.K.Chen, H.T.Chen; Numerical Heat Transfer, **14**, 343 **(1998)**.

[5] C.K.Chen, H.T.Chen, T.M.Chen; Comp.Methods Appl.Mech.Eng., **63**, 83 **(1987)**.

[6] C.K.Chen, Y.C.Yang; J.Eng.Sci., **24**, 569 **(1986)**.